International Orthopaedics (SICOT) (2016) 40:2163–2169
DOI 10.1007/s00264-015-3106-y

ORIGINAL PAPER

Fixation of a split fracture of the lateral tibial plateau with a locking screw plate instead of cannulated screws would allow early weight bearing: a computational exploration

Ion Carrera[1] · Pablo Eduardo Gelber[1,2] · Gaetan Chary[3,4] · Miguel A. González-Ballester[3,5] · Juan Carlos Monllau[2,6] · Jerome Noailly[3,4]

Received: 26 October 2015 / Accepted: 29 December 2015 / Published online: 16 January 2016

Abstract
Purpose To assess, with finite element (FE) calculations, whether immediate weight bearing would be possible after surgical stabilization either with cannulated screws or with a locking plate in a split fracture of the lateral tibial plateau (LTP).
Methods A split fracture of the LTP was recreated in a FE model of a human tibia. A three-dimensional FE model geometry of a human femur-tibia system was obtained from the VAKHUM project database, and was built from CT images from a subject with normal bone morphologies and normal alignment. The mesh of the tibia was reconverted into a geometry of NURBS surfaces. A split fracture of the lateral tibial plateau was reproduced by using geometrical data from patient radiographs. A locking screw plate (LP) and a cannulated screw (CS) systems were modelled to virtually reduce the fracture and 80 kg static body-weight was simulated.
Results While the simulated body-weight led to clinically acceptable interfragmentary motion, possible traumatic bone shear stresses were predicted nearby the cannulated screws. With a maximum estimation of about 1.7 MPa maximum bone shear stresses, the Polyax system might ensure more reasonable safety margins.
Conclusions Split fractures of the LTP fixed either with locking screw plate or cannulated screws showed no clinically relevant IFM in a FE model. The locking screw plate showed higher mechanical stability than cannulated screw fixation. The locking screw plate might also allow full or at least partial weight bearing under static posture at time zero.

Keywords Tibial plateau fractures · Finite element · Weight bearing · Interfragmentary motion · Bone fixation · Fracture fixation

✉ Ion Carrera
dr.carrera@orthopaedic-trauma.eu; icarrera@santpau.cat

[1] Orthopaedic Surgery Department, Hospital de la Santa Creu i Sant Pau, Universitat Autònoma de Barcelona, C/Sant Quintí 89, 08041 Barcelona, Spain

[2] ICATME-Hospital Universitari Quirón-Dexeus, Universitat Autònoma de Barcelona, Sabino de Arana 5-19, 08028 Barcelona, Spain

[3] Department of Communication and information Technologies (DTIC), Universitat Pompeu Fabra, Barcelona, Spain

[4] Institute for Bioengineering of Catalonia (IBEC), Barcelona, Spain

[5] ICREA, Pg. Lluis Companys 23, 08010 Barcelona, Spain

[6] Orthopaedic Surgery Department, Parc de Salut Mar, Universitat Autònoma de Barcelona, Barcelona, Spain

Introduction

Due to the specific geometry of the knee and the tibiofemoral joint forces, more than 60 % of the tibial plateau fractures affect its lateral column [1]. Most of these fractures of the lateral tibial plateau have a split pattern. Some of them also associate a depression of the articular surface. Surgical treatment is frequently accomplished with *ad minimum* fixation with percutaneous cannulated screws. However, some surgeons prefer plate fixation with locking screws, in order to achieve a more stable construct [2].

Post-operatively, a non-weight bearing period of six to eight weeks is recommended [1, 3]. This non-weight bearing period highly impairs the patient's functionality, which probably delays the final outcomes, and increases health-care costs. Finally, the absence of mechanical forces applied to the knee might also affect the articular cartilage [4, 5].

Few in vitro studies have measured the loads on surgically stabilized tibial plateau fractures. They have tested from about 300 N [6, 7] to a few thousands of Newtons [8, 9]. Hence, clear conclusions are often difficult to achieve in terms of an effective mechanical resistance of surgically stabilized fractures and in terms of the optimal fracture reduction technique. In general, experimental studies have considered the interfragmentary motions (IFM) to the displacement of the loading head, while neglecting the compliance of the whole experimental setup. Thus, those data cannot represent the biomechanics of the fracture per-se.

Conversely, a finite element (FE) method would allow not only detailed quantitative estimations of local IFM, but also the load distributions in both the simulated surgical implants and the surrounding bone. Finite element simulation-based loads predictions within tissues have also been reported as a promising model to understand the process of healing in bone fractures [10]. It has also been shown to potentially stand for good predictors of bone fracture [11, 12].

The objective of this study was to assess, with FE calculations, whether immediate weight bearing would be possible after surgical stabilization either with cannulated screws or with a locking plate in a simple fracture of the lateral tibial plateau. It was hypothesized that locking plate fixation would offer higher stability than cannulated screw fixation, and this stability would allow immediate weight bearing without clinical relevant IFM.

Materials and methods

A three-dimensional FE model geometry of a human femur-tibia system was obtained from the VAKHUM project database (http://www.ulb.ac.be/project/vakhum), and was built from computerized tomography images of a 99 years-old female of 155 cm and 55 kg. The subject had normal bone morphologies, and the femoro-tibial mechanical angle had a normal alignment. The mesh of the tibia was reconverted into a geometry of NURBS surfaces. A simple split fracture of the lateral tibial plateau was reproduced by using geometrical data from patient radiographs. The Polyax® tibial locked plating system (Biomet Inc, IN, USA) and a set of cannulated titanium 6.5 mm cancellous bone screws (Biomet Inc, IN, USA) were simulated. External shape of the Poliax plate was acquired with a three-dimensional metrology (Mitutoyo® Euro-C-A9166). A cloud of points was obtained with the software Metrolog XG 14.003 (Metrologic Group, France), and was then interpolated so as to obtain the entire geometry of the implant. The cannulated screws were directly modelled from the dimensions provided by the manufacturer (Biomet Inc). Both devices were virtually implanted into the fractured tibia geometry, according to commonly recommended positioning and alignment (Fig. 1a).

Implanted tibia models were then discretized into a structured meshed of hexahedral elements (Fig. 1b). For the femur, linear elements were used for both the implants and the tibia. The mechanical effect of the cortical bone was simulated through the juxtaposition of shell elements to the faces of the hexahedral elements at the bone model surface. For the tibia, a mean cortical thickness of 8 mm was calculated from the analysis of computerized tomography (CT) images from a 39 years old male and a 71 years old female patients. Informed consents were obtained from these two patients to use their data for study purposes. Thickness measurements were performed after segmentation with ITK-Snap 3.2.0 (http://www.itksnap.org/pmwiki/pmwiki.php) [13].

The bone was considered isotropic linear elastic. The cortical bone had a mean stiffness of 13 GPa, according to reported macroscopic experimental measurements on tibial bone samples [14]. A mean stiffness of 126 MPa was calculated for the trabecular bone according to a unique set of regional mechanical measurements on normal cadaveric specimens of the proximal tibia [15]. For the surgical devices, a 114 GPa stiff Ti 6Al 4 V material with a Poisson's ratio of 0.34 was simulated [16]. For the bone components, generic Poisson's ratios of 0.3 were chosen. The fracture was treated as a finite sliding contact problem with a direct boundary constraint that prevented surface penetration. The screws and the bone were considered perfectly bounded.

An axial force of 400 N pressed the femur model against the tibial plateau through the resolution of a frictionless local contact problem, simulating the weight of an 80 kg patient in bipedal stance (Fig. 2a). Along contact interfaces (Femur/Tibia, Femur/Fragment and Tibia/Fragment), normal efforts are transmitted, while surfaces can slip freely one over each other in the directions tangent to contact. IFM were calculated as the displacements between two nodes initially superimposed in the plane of the fracture, and six control points were chosen (Fig. 2b). The different contact reaction forces and the principal stresses transmitted to the bone were also calculated. CAD operations, pre- and post-processing were performed with Salome 7.5.1, and simulations used the Salome-Meca 2015.1 (Code Aster solver, EDF, France).

Results

The medial and lateral reaction forces on the tibial plateau were respectively 325 and 75 N with the Polyax®, and 367 and 33 N with the cannulated screws (Fig. 3). The reaction force between the fragment and the tibia was one order of magnitude higher with the cannulated screws than with the Polyax® device. In addition, while the lateral fragment was slightly compressed against the tibia model with the Polyax® plating system, a tendency to separate from the tibia with the cannulated screws was observed. Accordingly, the maximum IFM calculated with the cannulated screws was more than

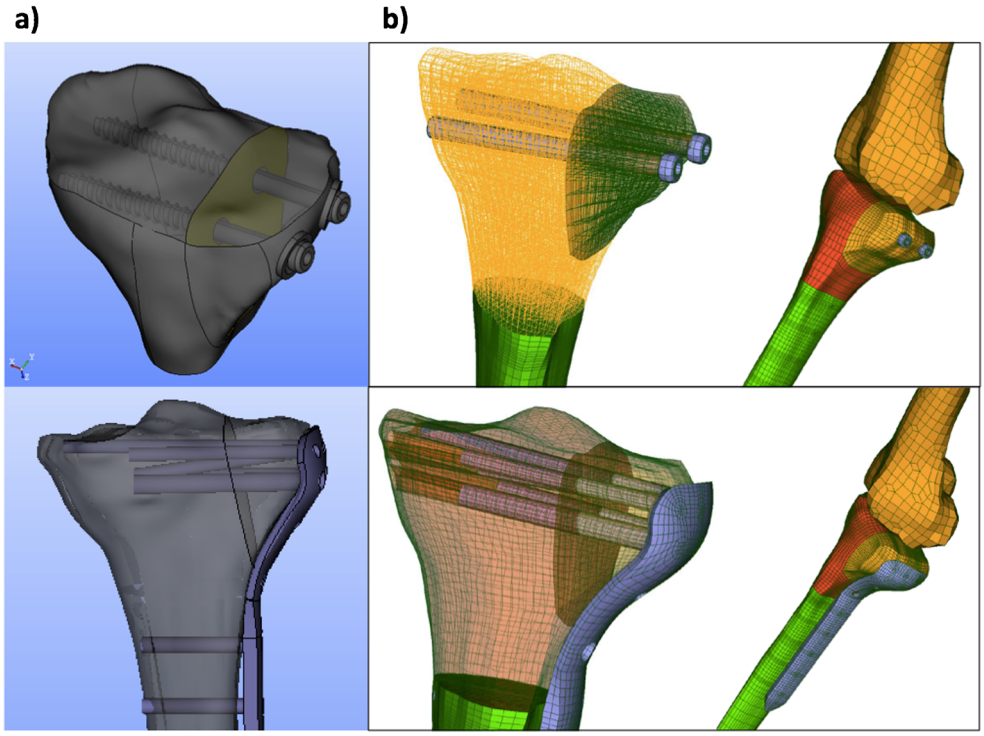

Fig. 1 Implanted models of the proximal tibia with the simulated split fracture of the lateral plateau (*top*: cannulated screws; *bottom*: Polyax® tibial locked plating system). **a**) Geometries. **b**) Finite element meshes

twice that calculated with the Polyax® (Fig. 4). However, the values did not overcome 0.03 mm.

With regard to the stresses transmitted to the trabecular bone, maximum shear stresses were 0.17 and 0.66 MPa with the Polyax® and the cannulated screws, respectively (Table 1).

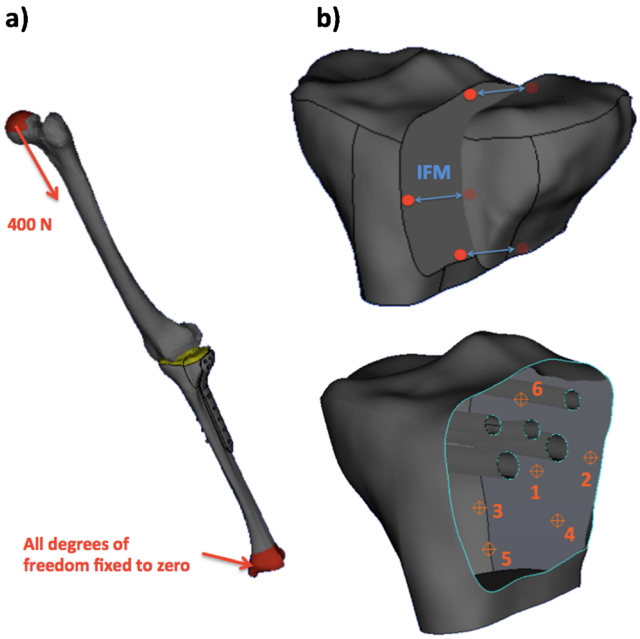

Fig. 2 **a**) Representation of the load boundary conditions imposed on the model (the contact area between the femur and the tibia appears in yellow). **b**) Calculation of the interfragmentary movement (IFM) — *top*: representation of the IFM as defined in this study – *bottom*: control points effectively used in the fracture plane to calculate the IFM

Maximum principal stresses were always one order of magnitude higher with the cannulated screws than with the Polyax®, and the largest computed values were 0.24 and 0.13 MPa in traction and compression respectively. Trabecular bone stresses tended to concentrate around the screws nearby the fracture plane with the Polyax®, while they showed a tendency to concentrate around the beginning of the screw thread with the cannulated screws (Fig. 5a). Maximum von Mises stresses within the simulated implants were generated by the contact with the cortical shell, with values of nearly 20 MPa for the Polyax® and 32 MPa for the cannulated screws (Fig. 5b). Figure 5c shows the possible relation between trabecular bone maximum shear stress, based on predictions and model approximations, and shear strength, which aims to illustrate the possible risk of fracture for each implanted model, as detailed in the Discussion.

Discussion

While the calculated simulations suggested that IFM were not a limitation for weight bearing loading after surgery, the bending of the tibia-fragment interface might transmit damaging shear stresses to the trabecular bone that surrounds the screws. From the current calculations and quantitative interpretations of the results, the risk of local bone failure for fixation with cannulated screws was particularly high. Further, the stresses in the cannulated screws were localized at the junction between the non-threaded and the threaded sections. Should this

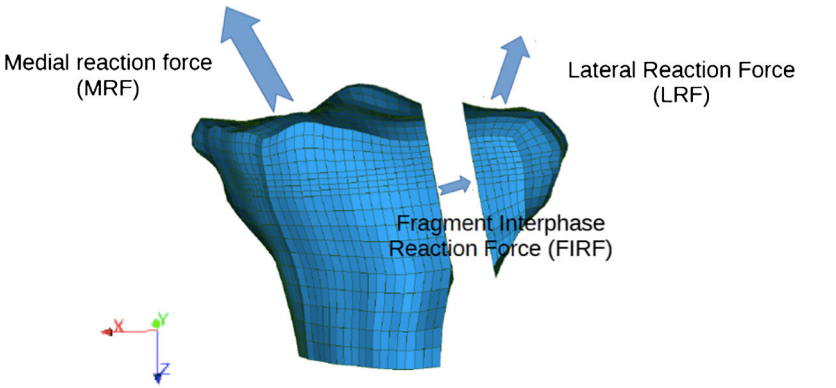

Fig. 3 Representation and values of the reaction forces calculated at the different contact interfaces of the model

	Polyax® system			Cannulated screws		
Direction	X	Y	Z	X	Y	Z
MRF (N)	-2.0	9.0	325.0	-33.0	8.8	367.0
LRF (N)	-18.0	9.0	75.0	7.5	13	33
FIRF (N)	2.4	0.0	0.0	-29.0	0.0	-4.0

junction be localized nearby the fracture plan, the risk of additional local bone damage would increase considerably. In contrast, the distal support provided by the Polyax® system to the fragment, and the redistribution over several screws of the internal mechanical support provided by the implant suggested the possibility to achieve a safer loading of the surgically stabilized fracture.

In terms of bone mechanics, calculation results indicated that shear stresses were the highest load components transmitted to the trabecular bone by the implant. These stresses resulted from the bending of the screws at the tibia-fragment junction, due to the force exerted by the femoral condyle onto the lateral tibia plateau. The shape of the Polyax® and the caudal support greatly helped to reduce this bending as it provided distal mechanical support to the fragment.

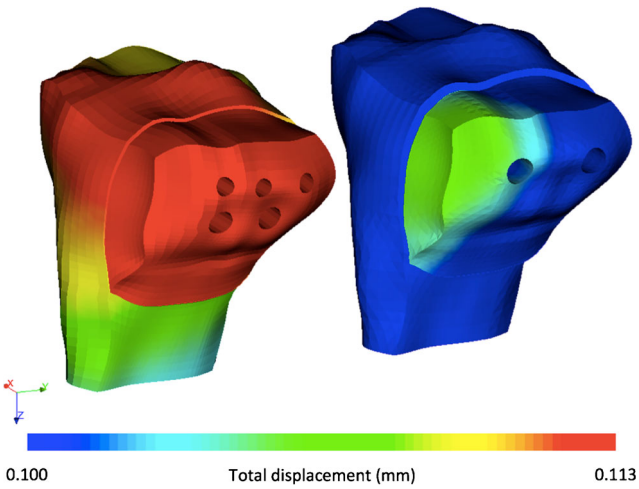

Fig. 4 Colour map of the total displacement values in the proximal part of the femur models with fracture and virtually treated with the Polyax® (*left*) and with the cannulated (*right*) screw systems (Deformations magnified x100)

In regards to the calculated bone stress in relation to bone strength, a homogenized Young's modulus of 126 MPa was adopted for the trabecular bone of the proximal tibia, leading to a homogenized compressive strength of about 3 MPa [15]. Unfortunately, little information is available about tibial bone strength under shear loads. Sanyal et al. [17] reported strong correlations between trabecular bone yield strength and volume fraction for a large number of bone samples, including proximal tibia bone samples. On one hand, these correlations associate a compressive strength of about 3 MPa to a bone volume fraction of about 0.1, which in turn would be associated to a shear strength of about 1.3 MPa. Independent measurements of the trabecular bone volume fraction in lateral proximal tibia gave values in a range of 0.14–0.24 [18]. These values suggest that the shear strength might vary from 2.4 to 5.8 MPa, according to the above-cited correlations [17]. Moreover, the regional stiffness of the trabecular bone may vary from 30 to 300 MPa in the proximal tibia, leading to similar variations in local compressive [15] strength and in shear strength [17]. Accordingly, a factor of safety of 10 might

Table 1 Maximum values calculated for the maximum principal stress (traction), minimum principal stress (compression), and maximum shear stress in the trabecular bone around the screws of the different simulated fixation systems

	Polyax® system	Cannulated screws
Maximum principal stress (MPa)	0.02	0.24
Minimum principal stress (MPa)	−0.04	−0.13
Maximum shear stress (MPa)	0.17	0.66

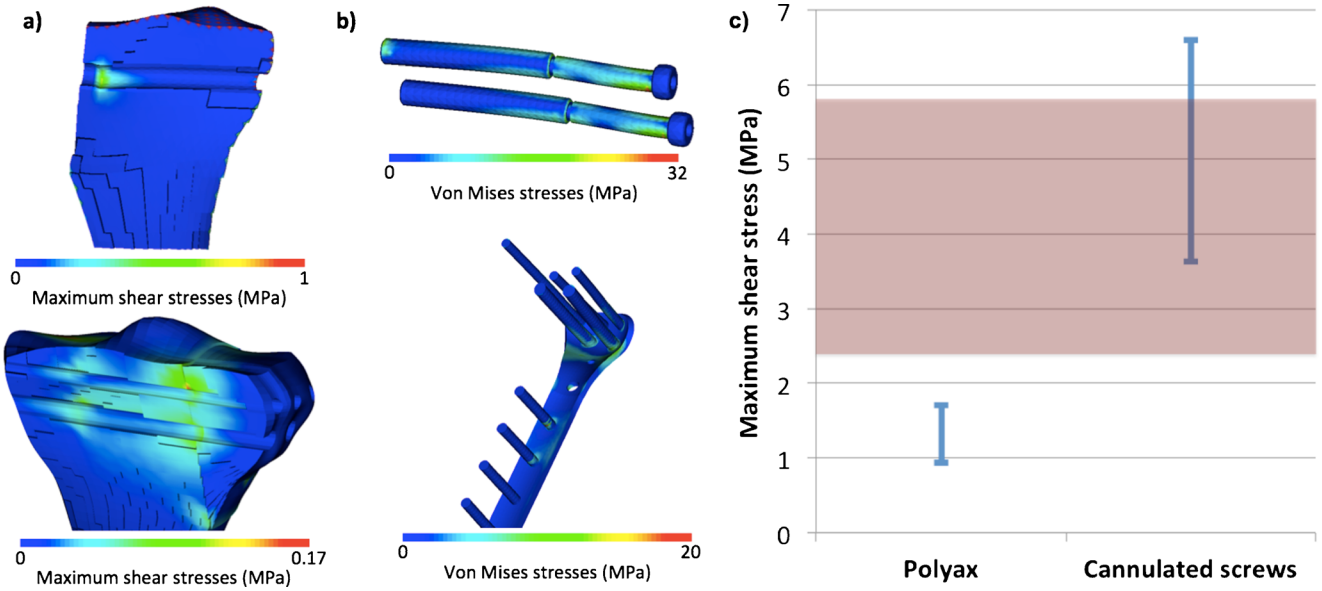

Fig. 5 Stress distributions in different parts of the deformed finite element models (deformations magnified x100). **a**) Model frontal cuts that shows the trabecular bone maximum shear stresses around the screws of the cannulated screw (*top*) and Polyax® (*bottom*) systems. (*Colour dots* at the cranial and lateral model periphery on the top illustration are postprocessing artefacts). **b**) Von Mises stresses in the virtually implanted devices. **c**) Estimated uncertainty on the maximum shear stress predictions and relation to the possible values of trabecular bone shear strength (see Discussion), as represented by the *colour box*

be applied to this bone mechanics analysis. While the maximum shear stress can vary from 0.17 to 1.7 MPa, such a rough estimation suggests a relatively low risk of bone fracture with the Polyax® system. Conversely, with the obtained calculated range of maximum shear stress from 0.66 to 6.6 MPa with the cannulated screw system, a substantially higher risk of bone fracture might be considered.

The axial stiffness of the implanted models ranged from about 2800 N/mm (Cannulated screws) to about 3300 N/mm (Polyax®), and the stiffness of the intact tibia model was superior to 3700 N/mm. Direct comparisons of the calculated IFM with the experimental data reported in the literature are difficult to achieve. On one hand, there are limited experimental studies that have focused on such comparisons. The found values in this study had the same order of magnitude to those reported by Karunakar et al. [19], who used the femoral condyles of a total knee prosthesis to load mechanically both intact tibia specimens, and specimen with replicated Schatzker type II plateau fractures: the measured stiffness of the intact specimens was of the order of 4000 N/mm, and that of the fractured specimen with surgical reduction was of the order of 2000 N. Unfortunately, the types of fixation explored in their experiments was different from the one used in the current study. Yet, it has been repeatedly reported that the type of fixation used to reduce split fractures of the tibial plateau had very limited influence on the post-operative stiffness or fixation strength [6, 7, 19, 20]. As far as the elastic deformation regime is considered, the IFM calculated in the present study were relatively low, independent of the type of fixation simulated. Actually, a difference of 0.02 mm was predicted between the maximum IFM respectively achieved with the Polyax® and the cannulated screws, which might be difficult to measure in vitro. If only the fragment is considered, the model predicted an apparent stiffness of the virtually reduced lateral plateau resulted to be about 2700 N/mm for the Polyax® and about 2600 N/mm for the cannulated screws. These values remained similar to those measured when the tibial plateau was loaded through the femoral components of total knee prostheses (2000–2600 N/mm) [19].

Overall, the maximum IFM achieved were far below the IFM threshold usually considered clinically (2 mm) to evaluate the success of the reduction of a split tibial plateau fracture [21]. The values calculated with the two models were inferior than 0.1 mm, which would be expected to largely favour processes of intramembranous fracture healing, according to the experimental mechanobiological data reported by Claes et al. [22]. These authors reported, however, that the size of the fracture gap has an important combined effect on both the capacity and type of fracture healing. In the models, we considered a perfect contact of the fracture surface (i.e. the gap was virtually nil), while some millimetres of gap might exist clinically. Still, gap size inferior to 1 mm would generally favour intramembranous healing [22]. Furthermore, the fracture model consisted in a mechanical discontinuity ruled by a frictionless contact problem: as soon as contact was established, the relative movement of the fragment did not depend on the pressure exerted by the implants but only on the stiffness of the bone-implant system, and on the respective directions of the reaction forces imposed by the implant. Hence, we can infer that this numerical approximation would

partly compensate the lack of consideration of the gap size effect.

As for the calculated force components, most of the boundary forces that simulated the static body weight were transmitted to the tibia model through the lateral plateau, according to its biomechanical role. With the Polyax® plate fixation, the reaction force on the lateral plateau stood for about 18 % of the total force, while the lateral plateau only bore 8 % of the total force after virtual fracture reduction with the cannulated screws. Such a difference can be attributed to the additional caudal support provided to the fragment by the Polyax® system, as shown by the absence of interfragmentary forces in the axial direction. Direct validation of the predicted force distributions between the lateral and medial plateau is not straightforward either. Several load patterns on the tibial plateau have been evaluated previously, either in cadaveric models as well as with motion tracking and inverse force calculations [23–25]. Remarkably, most of these studies have confirmed the higher frequency and/or higher magnitude of loads on the lateral over the medial plateau during the stance phase of a gait cycle. Finite element calculations performed with anatomically detailed knee models reported similar outcomes [26]. However, inverse dynamic analyses from captured body motion have consistently reported lateral plateau peak forces that are half the peak forces of the medial plateau [24, 25]. Certainly, our larger differences between lateral and medial plateau loads arose from the lack of consideration of the knee joint dynamics/complexity effects, especially in terms of forces of inertia and adduction coupled motions [24]. Arguably, the use of different assumption to solve a specific contact problem might also affect the reaction force results. In our case, the different parts of the model in contact were allowed to slide one over each other, but not to separate in the normal direction. On one hand, proper convergence of this numerical assumption was verified against simulations with no restriction on surface contact separation. On the other hand, our specific approach was advantageous in three different ways: 1) initial contact between femur and tibia (or fragment) was ensured without the need of simulating soft tissues, 2) since friction effects were neglected, our IFM values were probably overestimated, adding to the relative safety of our interpretations, 3) contact problem remained linear, leading to reduced CPU resources and calculations times.

The maximum von Mises stresses calculated in the implants can be directly compared to the maximum resistance of 795 MPa reported under axial traction for the simulated materials [16]. This comparison suggests that no mechanical damage would be expected in the implants because of the simulated body weight. This outcome is in agreement with the in vitro testing results reported by Parker et al. [6], who demonstrated that in split fractures of the lateral tibial plateau fixed with cannulated screws, no bending of the screws were observed even with loads as high as 900 N. In addition, the authors reported no screw pull-out, which supports the predictions of only local peak for the bone around the screws. Conversely, immediate screw pull-out at the beginning of failure should involve high stresses all along the screws.

This study suggests that plate fixation with a locking screw plate might allow full or at least partial weight bearing under static posture. It generally offers higher mechanical stability than cannulated screw fixation, though none of these fixation techniques led to calculate clinically relevant IFM. Importantly, the results of the bone stress calculation suggest that the safety margin would not allow applying several times the body weight, as it would occur with inertial effects [27]. One of the limitations of the study was that bone heterogeneity or quality was not considered on the locally calculated bone stresses, which might be critical and remains to be explored. Fragment size and number could be determinant for implant choice and results [28, 29], however we used the same bone quality and fragment size in order to reduce variability in our study. Local bone properties also relate to the femoro-tibial alignment [30], and combining calculations with patient-specific model geometries should be part of future assessments of immediate load bearing capacity after fracture reduction. For this purpose, population-based customization of FE models is both feasible and promising [31, 32].

Conclusions

Split fractures of the lateral tibial plateau fixed either with a locking screw plate or with cannulated screws showed no clinically relevant IFM in a FE model. Fracture fixation with a locking screw plate showed higher mechanical stability than cannulated screw fixation. The locking screw plate might also allow full or at least partial weight bearing under static posture at time zero.

References

1. Burdin G (2013) Arthroscopic management of tibial plateau fractures: surgical technique. Orthop Traumatol Surg Res 99:S208–S218
2. Ehlinger M, Adamczewski B, Rahmé M, Adam P, Bonnomet F (2015) Comparison of the pre-shaped anatomical locking plate of 3.5 mm versus 4.5 mm for the treatment of tibial plateau fractures. Int Orthop 39(12):2465–2471
3. Tscherne H, Lobenhoffer P (1993) Tibial plateau fractures. Management and expected results. Clin Orthop Relat Res 87–100
4. Eckstein F, Hudelmaier M, Putz R (2006) The effects of exercise on human articular cartilage. J Anat 208:491–512
5. Honkonen SE (1995) Degenerative arthritis after tibial plateau fractures. J Orthop Trauma 9:273–277
6. Parker PJ, Tepper KB, Brumback RJ et al (1999) Biomechanical comparison of fixation of type-I fractures of the lateral tibial

plateau. Is the antiglide screw effective? J Bone Joint Surg (Br) 81: 478–480
7. Boisrenoult P, Bricteux S, Beaufils P, Hardy P (2000) Screws versus screw-plate fixation of type 2 schatzker fractures of the lateral tibial plateau. Cadaver biomechanical study. Arthroscopy French Society. Rev Chir Orthop Reparatrice Appar Mot 86:707–711
8. Ratcliff JR, Werner FW, Green JK, Harley BJ (2007) Medial buttress versus lateral locked plating in a cadaver medial tibial plateau fracture model. J Orthop Trauma 21:444–448
9. Cift H, Cetik O, Kalaycioglu B et al (2010) Biomechanical comparison of plate-screw and screw fixation in medial tibial plateau fractures (Schatzker 4). A model study. Orthop Traumatol Surg Res 96:263–267
10. Anderson DD, Thomas TP, Campos Marin A et al (2014) Computational techniques for the assessment of fracture repair. Injury 45:997–1003
11. Van Den Munckhof S, Zadpoor AA (2014) How accurately can we predict the fracture load of the proximal femur using finite element models? Clin Biomech 29:373–380
12. Falcinelli C, Schileo E, Balistreri L et al (2014) Multiple loading conditions analysis can improve the association between finite element bone strength estimates and proximal femur fractures: a preliminary study in elderly women. Bone 67:71–80
13. Yushkevich PA, Piven J, Hazlett HC et al (2006) User-guided 3D active contour segmentation of anatomical structures: significantly improved efficiency and reliability. Neuroimage 31:1116–1128
14. Guo XE (2001) Mechanical properties of cortical bone and cancellous bone tissue. Bone Mech. Handb. Second Edi
15. Goldstein SA, Wilson DL, Sonstegard DA, Matthews LS (1983) The mechanical properties of human tibial trabecular bone as a function of metaphyseal location. J Biomech 16:965–969
16. ASTM F136 "Standard specification for wrought titanium-6aluminum-4vanadium ELI (extra low interstitial) alloy for surgical implant applications (UNS R56401)
17. Sanyal A, Gupta A, Bayraktar HH et al (2012) Shear strength behavior of human trabecular bone. J Biomech 45:2513–2519
18. Ding M, Dalstra M, Danielsen CC et al (1997) Age variations in the properties of human tibial trabecular bone. J Bone Joint Surg (Br) 79:995–1002
19. Karunakar MA, Egol KA, Peindl R et al (2002) Split depression tibial plateau fractures: a biomechanical study. J Orthop Trauma 16: 172–177
20. Koval KJ, Polatsch D, Kummer FJ et al (1996) Split fractures of the lateral tibial plateau: evaluation of three fixation methods. J Orthop Trauma 10:304–308
21. Haller JM, O'Toole R, Graves M, et al. (2015) How much articular displacement can be detected using fluoroscopy for tibial plateau fractures? Injury
22. Claes LE, Heigele CA, Neidlinger-Wilke C, et al. (1998) Effects of mechanical factors on the fracture healing process. Clin Orthop Relat Res S132–S147
23. Wang H, Chen T, Torzilli P et al (2014) Dynamic contact stress patterns on the tibial plateaus during simulated gait: a novel application of normalized cross correlation. J Biomech 47:568–574
24. Hurwitz DE, Sumner DR, Andriacchi TP, Sugar DA (1998) Dynamic knee loads during gait predict proximal tibial bone distribution. J Biomech 31:423–430
25. Lin YC, Walter JP, Banks SA et al (2010) Simultaneous prediction of muscle and contact forces in the knee during gait. J Biomech 43: 945–952
26. Adouni M, Shirazi-Adl A (2014) Evaluation of knee joint muscle forces and tissue stresses-strains during gait in severe OA versus normal subjects. J Orthop Res 32:69–78
27. Kutzner I, Trepczynski A, Heller MO, Bergmann G (2013) Knee adduction moment and medial contact force-facts about their correlation during gait. PLoS One 8:8–15
28. Chang SM, Hu SJ, Zhang YQ, Yao MW, Ma Z, Wang X, Dargel J, Eysel P (2014) A surgical protocol for bicondylar four-quadrant tibial plateau fractures. Int Orthop 38(12):2559–2564
29. Li Q, Zhang YQ, Chang SM (2014) Posterolateral fragment characteristics in tibial plateau fractures. Int Orthop 38(3):681–682
30. Thorp LE, Wimmer MA, Block JA et al (2006) Bone mineral density in the proximal tibia varies as a function of static alignment and knee adduction angular momentum in individuals with medial knee osteoarthritis. Bone 39:1116–1122
31. Prendergast PJ, Galibarov PE, Lowery C, Lennon AB (2011) Computer simulating a clinical trial of a load-bearing implant: an example of an intramedullary prosthesis. J Mech Behav Biomed Mater 4:1880–1887
32. Taddei F, Palmadori I, Taylor WR et al (2014) Safety factor of the proximal femur during gait: a population-based finite element study article. J Biomech 47:3433–3440